Study on the Influence of Neutron Irradiation on High-power Thyristor Device in Fusion Environment*

Wei Tong,[1] Meng Xu,[2,3,†] Hua Li,[2,‡] Zhi-Quan Song,[2] and Bo Chen[1]

[1]*School of Electrical Engineering and Automation, Hefei University of Technology, Hefei 230009, China*
[2]*Institute of Plasma Physics, Hefei Institutes of Physical Science, Chinese Academy of Sciences, Hefei 230031, China*
[3]*University of Science and Technology of China, Hefei 230026, China*

Due to its good economy and applicability, high-power thyristor device is widely used in power supply systems of large fusion devices. The high-dose neutrons produced by Deuterium-Tritium (D-T) fusion reactions will irradiate the thyristor for a long time, which will lead to the change of the electrical characteristics of the thyristor, and may eventually cause irreversible damage. In this paper, the thyristor switch of the commutation circuit in Quench Protection System (QPS) of fusion device is regard as the study object. The relationship between the internal physical structure and the external electrical parameters of irradiated thyristor is established. Then, a series of targeted thyristor physical simulations and neutron irradiation experiments are carried out to verify the correctness of the theoretical analysis. In addition, the effect of irradiated thyristor electrical characteristic changes on the whole QPS is studied by accurate simulation, which provides valuable guidance for the maintenance and renovation of QPS.

Keywords: Fusion device, Neutron Irradiation effects, Thyrisor, Quench protection

I. INTRODUCTION

Tokamak is an experimental device for the development of nuclear fusion energy, in which the most easily achieved fusion reaction is Deuterium-Tritium (D-T) fusion, whose reaction formula is shown in Eq. (1) [1, 2]. When D-T fusion reaction occurs in Tokamak, about 80% of the energy will be released in the form of 14.1 MeV fast neutrons [3–5]. Nowadays, Tokamak is still in the experimental exploration stage, and some windows and channels need to be set up for observation, which may lead to an increase in neutron irradiation flux in fusion environment. Taking the ITER Tokamak as an example [6], when the 500 MW D-T fusion reaction experiment is carried out, the number of fast neutrons produced by the plasma is $1.78 \times 10^{20} n \times s^{-1}$ [7]. After installing the shielding layer and considering the neutron attenuation, the calculated neutron flux rate in the whole host hall is still up to $10^5 n \times cm^{-2} \times s^{-1}$, which is far great than the safety threshold and has drastic impacts on the performance of the electrical devices around Tokamak [8, 9].

$$\mathrm{D} + \mathrm{T} \rightarrow \mathrm{n}\,(14.1\mathrm{MeV}) + {}^4\mathrm{He}\,(3.5\mathrm{MeV})\,, \qquad (1)$$

Quench Protection System (QPS) is usually designed to ensure the safety of the superconducting magnet in Tokamak [10, 11], in which thyristors are commonly used as the trigger unit of the commutation circuit, as shown in Fig. 1 [12, 13]. QPS works as follows: when superconducting magnet in normal operation condition, the current flows through ByPass Switch (BPS). Once quench occurs, BPS quickly opens, and the magnet current is transferred to Vacuum Circuit Breaker (VCB) by the arc voltage. Then the thyristors turn on, a pulse current generated by charged capacitor C and pulsed inductor L, to force the current in VCB down to zero [14, 15]. Finally, the magnet current is transferred to Discharge Resistor (DR) and the energy stored in magnet is constantly consumed until to zero.

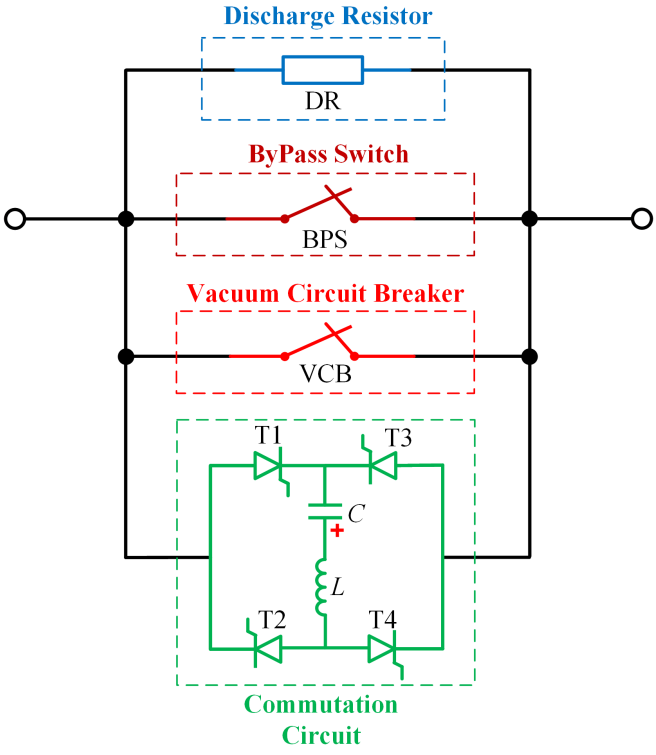

Fig. 1. (Color online) The circuit topology of QPS.

To effectively protect the superconducting magnetic coils

* Supported by the Fundamental Research Funds for the Central University under Grant JZ2023HGTA0182 and the Comprehensive Research Facility for Fusion Technology Program of China under Grant 2018-000052-73-01-001228

† Corresponding author, meng.xu@ipp.ac.cn
‡ Corresponding author, lihua@ipp.ac.cn

in the fusion device, the QPS needs to respond as quickly as possible. To ensure the QPS can do this, it should be located as closely as possible to the magnetic coils. Unfortunately, this is also where there is a high fast neutron flux rate, thus we likely cannot avoid neutron damage. The typical layout of fusion device and irradiation nephogram are shown in Fig. 2 [8, 9]. If the thyristor switch is damaged due to neutron irradiation and cannot operate normally, the current would not be interrupt quickly by VCB with the help of the auxiliary pulse current, which resulting in the failure of QPS and the destroy of superconducting magnet [16].

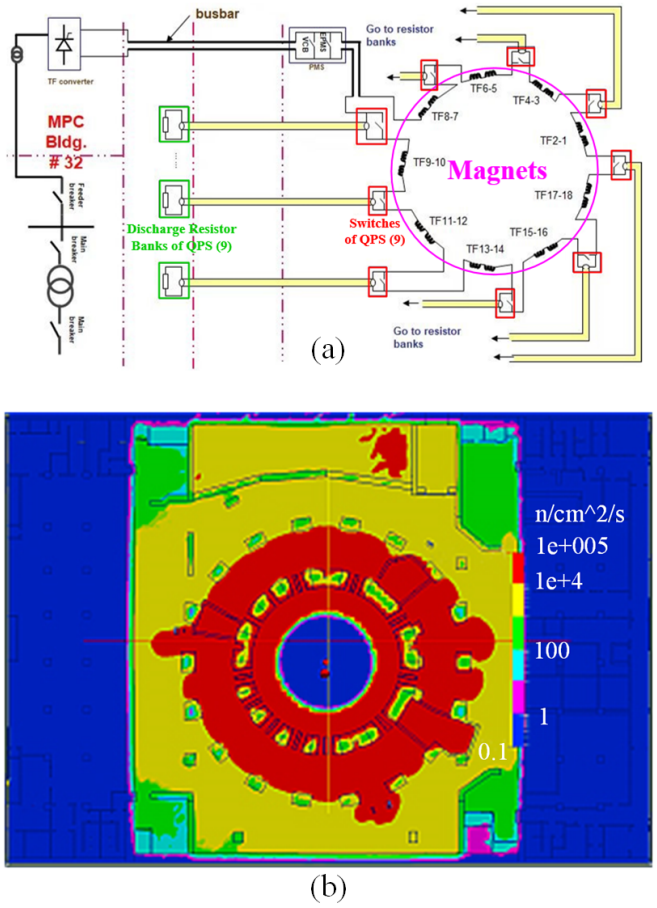

Fig. 2. (Color online) Typical layout of fusion device and irradiation nephogram. (a) Typical layout of fusion device. (b) Total Neutron Flux (TNF) caused by plasma in host hall, the max TNF is $10^5 n \times cm^{-2} \times s^{-1}$.

Since ITER takes the D-T fusion route, neutron irradiation damage is an issue that must be considered. More previous studies are focused on the main structural materials of fusion reactor, such as the First Wall, Blanket Modules and Divertor [17–19]. Gradually, ITER realized the threat of neutron irradiation to auxiliary equipment, and conducted irradiation calculation, established exposure limits and provided mitigation measures [8, 20, 21]. Researchers have carried out radiation reliability analysis on the basis of ITER guidelines, but it is far from sufficient, especially for high-power thyristors.

Semiconductor damage via high energy neutron irradiation is a topic not only of interest in the context of Tokamaks and Stellarators, but also in the context of spacecraft and satellites, where the electronics are similarly bombarded with a complex mix of high energy particles. [22–24]. Currently, in literature, the displacement damage effect and total ionization effect occurred in electronics and few power device have been separately studied at macro and micro levels. However, as the particularity of fusion neutron irradiation environment and the requirement for effective irradiation reinforcement, the relationship between internal physical structure changes and external electrical characteristic changes should be deeply studied and accurately built.

The neutron irradiation damage and internal physical structure change of semiconductor devices are mainly carried out by experiments. S. Yue *et al.* studied the synergistic effect of electrical stress and neutron irradiation on silicon carbide power MOSFETs. The defects in the devices were characterized by the Low Frequency Noise (LFN) and Deep-Level Transient Spectrum (DLTS) methods [25]. R. Chen *et al.* carried out the Displacement Damage Dose (DDD) and Total Ionization Dose (TID) irradiation experiments with the 14.1 MeV neutron high-voltage multiplier and 60Co gamma-ray to study the synergistic effect of TID and DDD in neutron irradiated GaN HEMT [26]. However, the change relationships between various physical parameters and electrical characteristics of semiconductor devices need to be further studied.

On the other hand, F. Ravotti and J. Mekki studied I-V characteristic of PIN photodiode under 1 MeV neutron irradiation at European Organization for Nuclear Research (CERN) [27, 28]. Through a lot of irradiation experiments and tests, the relationship curves of forward conduction voltage drop and leakage current under different neutron flux are obtained. C. Liu *et al.* studied the influence of fast neutron irradiation on the high di/dt switching characteristics of the pulse power supply Insulated Gate Triggered Thyristor (IGTT) through experiments [29]. The simulation and test results indicate that the neutron irradiation bring significant decrease of threshold voltage and on-state voltage of IGTT. However, the studies did not give a detailed description and exploration of the physical causes leading to the electrical characteristic changes.

In this paper, we focus on studying the characteristics change of the thyristor switch within the fusion device's QPS shown in Fig. 1. The internal physical structure changes of the thyristor caused by neutron irradiation are introduced firstly to obtain the possible physical parameters which may cause the electrical characteristic changes. Then, in view of various key electrical parameters of thyristor, the relationship between physical and electrical characteristics of thyristor after neutron irradiation is theoretically analyzed. Also, a series of targeted thyristor physical simulations and neutron irradiation experiments are carried out to verify the correctness of the theoretical analysis results. Furthermore, the effect of irradiated thyristor characteristic changes on the whole QPS is also been studied by the performance simulation. The study not only build a clear relationship between the changes of physical and electrical characteristics of the neutron irradi-

ated thyristor, but also provides a valuable guideline for the maintenance and renovation of QPS.

II. THEORETICAL DISCUSSION OF THE RELATIONSHIP BETWEEN PHYSICAL AND ELECTRICAL CHARACTERISTICS CHANGE OF THE THYRISTOR AFTER NEUTRON IRRADIATION

A. Damage Mechanism Analysis of Physical Characteristics of Thyristor after Neutron Irradiation

Since neutrons are electrically neutral and have very strong penetrability, it can be sufficiently close to the atomic nucleus of the lattice atom of the material to be radiated and collide with the atomic nucleus elastically [30, 31]. The lattice atom gets energy in the collision process, thus leaving its normal lattice position and becoming an interstitial atom in the lattice, and leaving a vacancy in its original position. If the vacancy and interstitial atom are still within the coulomb force field of its elastic force field, recombination can be occurred. If the force field is exceeded, the interstitial atoms will not recover, thus causing atomic displacement. The production process of vacancy and interstitial atom is shown in Fig. 3.

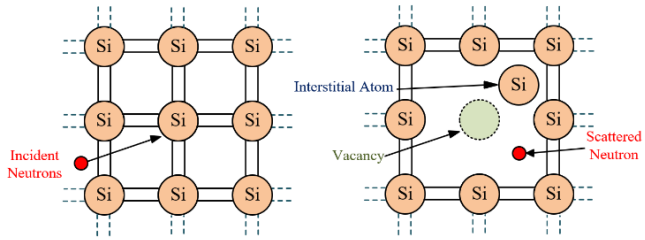

Fig. 3. (Color online) The production mechanism of vacancy and interstitial atom in Si material.

Vacancies can be combined with adjacent atoms or with vacancies. Vacancies can also be moved to the vicinity of doping to form vacancy impurity complexes, so that doping do not participate in conductivity, thus changing the density of doping. The displacement of a single atom forms a simple defect, called the Frenkel Defect [32]. If the incident neutrons energy is large enough, the displaced interstitial atoms will get enough energy. The collision of such interstitial atoms will displace a large number of atoms in the lattice, forming a large defect cluster.

Literature [33] indicates that when the incident neutron energy is 1 MeV, the average energy obtained by the initially displaced atom is 72.5 keV, while the displacement threshold for a Si atom is 15 eV. The D-T reaction produces a neutron energy of 14.1 MeV, which is about 1 million times the Si atomic shift threshold, thus obviously has a great impact on Si materials. In addition, it also shows that a defect group generated by a 1 MeV neutron can include about 200 to 1000 displaced lattice atoms, Although the collision cross section between neutron and lattice atom is only between $10^{-23}cm^2$ and $10^{-24}cm^2$, the energy transferred to the lattice atom by collision is quite large, a series of lattice atoms can eventually be displaced.

Semiconductor materials have three microscopic physical parameters, namely minority carrier lifetime τ, pure doping density n and mobility μ. Neutron irradiation introduces defects and defect cluster in the semiconductor, thus changing the three microscopic physical parameters and changing almost all parameters of the semiconductor device.

Defects formed by neutron irradiation can introduce additional energy levels into the forbidden band of semiconductor materials, which increases the chance of recombination of minority carriers and majority carriers, increases the recombination rate, and thus reduces the minority carrier lifetime. The relationship between neutron flux and the minority carrier lifetime is given below.

$$\frac{1}{\tau(\phi)} = \frac{1}{\tau(0)} + k_\tau \times \phi, \tag{2}$$

Where $\tau(0)$ and $\tau(\phi)$ are the minority carrier lifetime before and after neutron irradiation, k_τ is the minority carrier lifetime damage coefficient of semiconductor materials, ϕ is the neutron flux.

As thyristor is a kind of semiconductor device with minority carriers as conductive mechanism, thus minority carrier lifetime damage will greatly affect the performance of the device.

Beside this, neutron irradiation also reduces the doping density of the semiconductor materials, which called carrier removal effect. The relationship between neutron flux and the doping density is given below.

$$n(\phi) = n(0) - \frac{\Delta n}{\Delta \phi} \times \phi, \tag{3}$$

Where $n(0)$ and $n(\phi)$ are the doping density before and after neutron irradiation, $\Delta n/\Delta\phi$ is the carrier removal rate, and ϕ is the neutron flux.

Also, when neutron irradiation introduces defects in semiconductor materials, these defects can be used as the scattering center of carriers, effectively reducing the mobility of carriers. The influence of these neutron irradiation on mobility can be expressed as

$$\frac{1}{\mu(\phi)} = \frac{1}{\mu_{ID}} + \frac{1}{\mu_L} + \frac{A_t \times [1 - \exp(\varepsilon_T - \varepsilon_f)/kT]}{B_t}\phi, \tag{4}$$

Where $\mu(\phi)$ is the mobility of carriers after neutron irradiation, μ_{ID} is the mobility due to stray atom scattering, μ_L is the mobility due to collision with thermal vibration lattice, A_t and B_t are the coefficients, ε_T and ε_f are the defect level and Fermi level respectively, k is Boltzmann constant, T is thermodynamic temperature, and ϕ is the neutron flux.

B. Establishment of Relationship between Physical and Electrical Characteristics Change after Neutron Irradiation

As thyristor has longer lifetime, more reliability, less maintenance and high rated power capability compared to other semiconductor devices, so it becomes the first choice for QPS in Tokamak superconducting system.

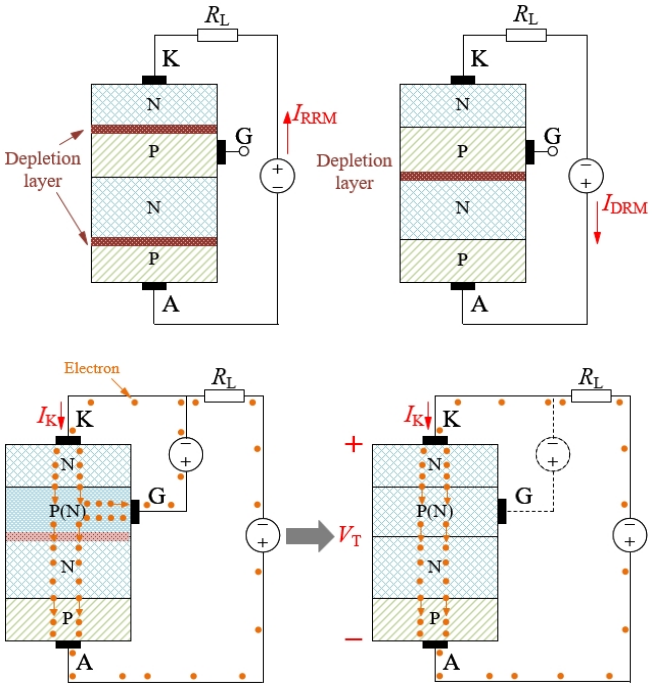

Fig. 4. (Color online) Internal structure diagram of thyristor. (a) Blocking state. (b) Conducting state.

Thyristor is composed of P-type and N-type semiconductor alternately [34]. As shown in Fig. 4, the depletion layer is formed at the junction of P-type and N-type semiconductor. If there is no external power supply to the gate of thyristor, there will always be at least one reverse biased depletion layer regardless of the voltage direction of the external circuit, which are shown in Fig. 4(a). If the thyristor gate is applied by an additional voltage, which is called gate trigger, a large number of electrons will be injected into P-region of the thyristor, and P-region eventually become N-region which will cause the depletion layer width gradually decrease and eventually almost disappear as shown in Fig. 4(b). As the injected electrons have already entered N-region, even though the thyristor gate is not applying additional voltage, it can still maintain the conducting state.

Hence, both blocking and conducting state of thyristor after neutron irradiation can be analyzed by simplifying it to PN diode.

1. *Blocking Characteristic*

The blocking charactersitic of thyristor is actually an expression of the reverse current of PN junction under reverse voltage, which can be divided into two conditions given in Fig. 4(a). Hence, the forward leakage current I_{DRM} and the reverse leakage current I_{RRM} are the most two crucial parameters to evaluate the blocking characteristic of thyristor. Fig. 5 shows the change of PN junction barrier region with reverse bias. When the applied electric field E is in the same direction as the self-built electric field E_0, the electric field in the depletion layer is strengthened. The enhancement of electric field makes the barrier region change in two ways: first, the barrier region becomes wider, and second, the barrier height increases.

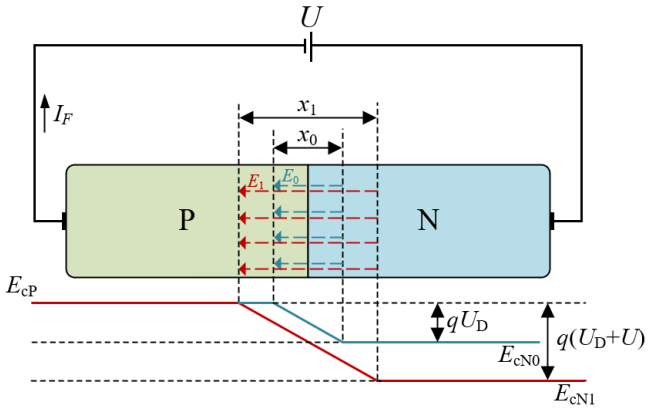

Fig. 5. (Color online) The change of PN junction barrier region with reverse bias.

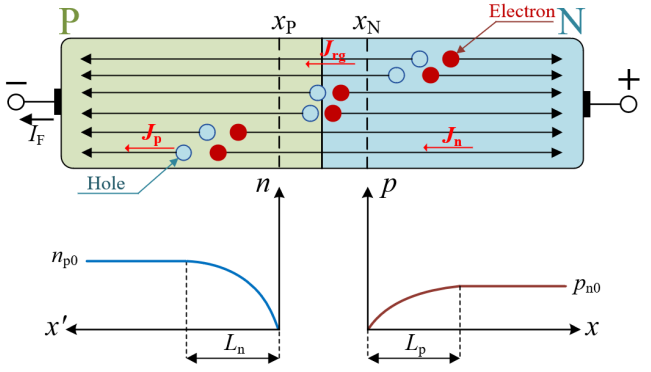

Fig. 6. (Color online) The diagram of reverse current generation and minority distribution.

Meanwhile, the balance between diffusion and drift of the carriers is broken by the growth of the barrier region, and drift plays a dominant role. Therefore, the electrons at the boundary of the P-region could be pulled to the N-region, and the holes at the boundary of the N-region could be pulled to the P-region. In the meantime, the electrons in the P-region and the holes in the N-region will run to the boundary to supplement, thus forming the reverse current I_F, which is directed

from the N-region to the P-region, as shown in Fig. 6. However, since there are few electrons in the P-region and holes in the N-region, the reverse current I_F is very small.

In the case of ignoring the recombination of electrons and holes in the barrier region, the current density J through the PN junction can be considered as the sum of the hole diffusion current density $J_p(x_N)$ passing through the x_N, the electron diffusion current density $J_n(x_P)$ passing through the x_P [34].

$$J = J_p(x_N) + J_n(x_P), \tag{5}$$

$J_p(x_N)$ could be calculated by the following equations if the hole and electron density distribution are obtained.

$$J_p(x_N) = -qD_p \frac{d\Delta p_n(x)}{dx}\bigg|_{x=x_N}, \tag{6}$$

Where $d\Delta p/dx$ are the hole density gradient, D_p is the hole diffusion coefficient.

If the P and N regions are long enough, the non-equilibrium carrier concentration in the PN junction should be distributed exponentially.

$$\Delta p_n(x) = [p_n(x_N) - p_{n0}] \exp\left(\frac{x_N - x}{L_p}\right), \tag{7}$$

Where L_p is the hole diffusion length.

$$L_p = \sqrt{D_p \tau_p}, \tag{8}$$

Also

$$p_n(x_N) = p_{n0} \exp\left(\frac{qU}{kT}\right), \tag{9}$$

Where p_{n0} is the equilibrium minority carrier concentration in N-region, U is the applied reverse voltage. Hence, $J_p(x_N)$ could be calculated by the following equation.

$$J_p(x_N) = \frac{qD_p p_{n0}}{L_p}\left[\exp\left(\frac{qU}{kT}\right) - 1\right], \tag{10}$$

By the same token,

$$J_n(x_P) = \frac{qD_n n_{p0}}{L_n}\left[\exp\left(\frac{qU}{kT}\right) - 1\right], \tag{11}$$

Consequently,

$$J = \left(\frac{qD_n n_{p0}}{L_n} + \frac{qD_p p_{n0}}{L_p}\right)\left[\exp\left(\frac{qU}{kT}\right) - 1\right], \tag{12}$$

$$I_F = AJ = A\left(\frac{qD_n n_{p0}}{L_n} + \frac{qD_p p_{n0}}{L_p}\right)\left[\exp\left(\frac{qU}{kT}\right) - 1\right], \tag{13}$$

Where A is PN junction cross-sectional area. As U approaches negative infinity, $\exp(qU/kT)$ approaches 0.

$$I_F = -A\left(\frac{qD_n n_{p0}}{L_n} + \frac{qD_p p_{n0}}{L_p}\right) = -I_0, \tag{14}$$

Hence, the I_F would increase as the carriers' lifetime τ_p and τ_n would be greatly shortened after neutron irradiation. In addition, as for silicon PN junction, the recombination current density J_{rg} in barrier region also plays a crucial role in the reverse current. After neutron irradiation, the number of recombination centers in the barrier region of PN junction increases, and the carrier generation rate increases, which leads to the rise of recombination current.

As a result, after neutron irradiation the reverse current I_F in PN junction would be increased, which will result in the increase of forward leakage current I_{DRM} and reverse leakage current I_{RRM} of irradiated thyristor.

2. *Conducting characteristic*

The conducing characteristic of semiconductor can be characterized by the on-state resistance or on-state voltage drop U_{TM}. The lower the U_{TM}, the better the high current performance of the device, which is a significant parameter of the semiconductor applied in QPS of fusion device as the extremely high current breaking requirement of superconducting magnet.

In order to have high working voltage capability, the substrate resistivity of the PN junction diode is generally high, that is, the substrate doping concentration is low and the substrate region is wide. Therefore, the defects caused by neutron irradiation led to carrier removal effect in semiconductor material is more apparent, resulting in plenty of conductive carrier constrain and not participate in conduction. Hence, the resistivity increases, so as to increase the conducting voltage of PN junction.

According to the above analysis, the conducting characteristic of thyristor can be analyzed by simplifying it to PN diode. The on-state voltage drop of PN diode U_{TM} can be divided into two parts: one is the junction voltage U_j formed by the internal electric field, and the other is the voltage related to the substrate epitaxial layer U_b, U_j and is very small and negligible.

$$U_T = U_j + U_b \approx U_b, \tag{15}$$

According to the literature [33], U_b can be expressed as the following equation.

$$U_b = \frac{Iw_d}{A\sigma_p}, \tag{16}$$

Where w_d is the base region width of PN junction, σ_p is the conductivity of P-region.

The conductivity of irradiated material can be derived as

$$\sigma(\phi) = \sigma(0) e^{-\alpha\phi}, \tag{17}$$

$$\ln \frac{\sigma(0)}{\sigma(\phi)} = \alpha\phi, \tag{18}$$

When ϕ approaches 0,

$$\alpha = \frac{1}{\sigma(0)} \times \left.\frac{d\sigma(\phi)}{d\phi}\right|_{\phi\to 0}, \tag{19}$$

As

$$\sigma = q\mu p, \tag{20}$$

Where μ is majority carrier mobility of PN diode, and p is base doping concentration of PN diode.

Then

$$R = \left.\frac{dp}{d\phi}\right|_{\phi\to 0}, \tag{21}$$

$$\alpha = \frac{q\mu(\phi)}{\sigma(0)} \times R, \tag{22}$$

$$\ln \frac{\sigma(0)}{\sigma(\phi)} = \frac{q\mu(\phi)}{\sigma(0)} \times R\phi, \tag{23}$$

Where R is carrier removal rate.

According to Eq. (16)

$$\sigma = \frac{Iw_d}{AU_b}, \tag{24}$$

Substitute Eq. (24) into Eq. (23)

$$\frac{U_b(\phi)}{U_b(0)} = \exp\left[\frac{q\mu(\phi)}{\sigma(0)} \times R\phi\right] > 1, \tag{25}$$

It can be concluded from the above analysis that U_b will increase as majority carrier removal effect in the PN junction. In addition, the change of the irradiated thyristor on-state voltage drop U_{TM} is determined by the irradiation intensity, which will be discussed by further neutron irradiation simulation and experiment.

3. *Reverse Recovery Characteristic*

Reverse recovery is "turning off" a thyristor after it has been in a conducting state, and that the time taken for it to switch from conducting to blocking state is critical and needs to be minimised. Usually neutron damage decreases reverse recovery time, this is because the minority carrier lifetime of the thyristor is significantly shortened after irradiation.

The typical reverse recovery current waveform is shown in Fig. 7. I_P is the peak value of the forward current. $t_s = t_2 - t_1$ is the time of the reverse current grows from zero to maximum value I_{RM}, which is called storage time. $t_f = t_3 - t_2$ is the time of the current drop from I_{RM} to $0.1I_{RM}$, which is called fall time. The total reverse recovery time is $t_{rr} = t_s - t_f$, and Q_{rr} is the reverse recovery charge [35].

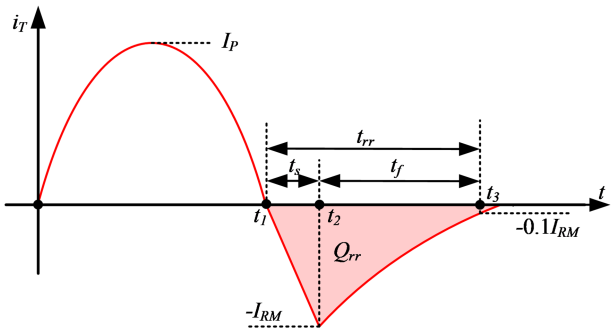

Fig. 7. (Color online) The typical reverse recovery current waveform.

When the thyristor is in conducting state, most of the charges stored in the base region, which are formed by the minority carrier. The charge continuity equation is given as follow,

$$i_T(t) = \frac{dQ}{dt} + \frac{Q}{\tau}, \tag{26}$$

Where $i_T(t)$ is the current flow through the thyristor, Q is the stored charge in base region, τ is the minority carrier lifetime.

The thyristors in QPS play the role of the trigger unit of the commutation circuit composed of the pulsed inductor L and the charged capacitor C. To simplify the analysis, the forward conducting current is considered to be sinusoidal current, $i_T(t) = I_P \sin wt$. According to Eq. (26), it can be obtained that

$$Q(t) = \frac{K_0 I_P \tau}{1 + w^2\tau^2}\left(w\tau e^{-t/\tau} + \sin wt - w\tau\cos wt\right), \tag{27}$$

Where K_0 is the current gain of the thyristor.

At t_1, the charge $Q(t_1)$ can be calculated by using Eq. (27)

$$Q(t_1) = \frac{K_0 I_P w\tau^2}{1+w^2\tau^2}\left(1+e^{-\pi/w\tau}\right), \quad (28)$$

When the forward current drops to zero, there are still large number of non-equilibrium carriers in thyristor, which will be dissipated by the way of sweeping out and recombination. At time t_2, the current reaches I_{RM}, and the thyristor begins to recover the reverse blocking capability. At this time, only a small amount of stored charge remains in the base region. Those charge will disappear by the way of recombination, which is classified as low injection condition. Actually, high-power semiconductor devices generally work under large injection condition, so it can be approximately considered that $Q(t_2) = 0$. According to Eq. (27), it can be calculated that

$$\sin wt_2 = w\tau\left(\cos wt_2 - e^{-t_2/\tau}\right), \quad (29)$$

As $t_2 = t_1 + t_s = \pi/w + t_s$, $wt_2 = \pi + wt_s$. Also, wt_s is far less than $\pi/2$, so wts approximately considers to be zero. Then, it could be deduced that $\sin wt_s \approx wt_s$, $\cos wt_s \approx 1$, therefore,

$$\sin wt_2 = \sin(\pi + wt_s) = -\sin(wt_s) \approx -wt_s, \quad (30)$$

$$\cos wt_2 = \cos(\pi + wt_s) = -\cos(wt_s) \approx -1, \quad (31)$$

Approximating Eq. (29), the expression of t_2 can be obtained

$$t_s \approx \tau\left(1+e^{-t_2/\tau}\right), \quad (32)$$

t_2 is much longer than τ, so

$$t_s \approx \tau, \quad (33)$$

Then, the maximum reverse current I_{RM} can be expressed by the following equation

$$I_{RM} \approx k(t_2 - t_1) = k\tau, \quad (34)$$

Where k is the forward current change rate at t_1 point.

On the basis of above analysis, it can be concluded that after high-dose neutron irradiating the thyristor, which reduces the minority carrier lifetime τ, the reverse recovery characteristics will have significant changes. According to Eq. (33) and Eq. (34), the stored time t_s and the maximum reverse current I_{RM} will decreases with the reduction of τ, which means that the total turn-off time of the semiconductor t_{rr} will be shorten as the result of high-dose neutron irradiation. Also, the reverse recovery charge Q_{rr} will have a sharp decrease after irradiation.

III. NEUTRON IRRADIATION SIMULATION

To verify the correctness of the above theoretical analysis of the thyristor damage mechanism under fusion neutron irradiation, a qualitative verification through material and device level simulation based on simplified thyristor model is necessary. The idea of simulation in this paper is that after neutron irradiation, the lattice of the device material is damaged, and the defects introduce additional energy levels, which will affect the electrical characteristics of the device. Therefore, two types of defects are mainly considered in this paper, namely, donor defects, characterized by E_C-0.12 eV, and acceptor defect, characteristic E_V+0.21 eV.

APSYS, as an advanced semiconductor device physical model simulation software, is used for simulation in this paper. The thyristor is an extremely complex device, and its designs are often patented and proprietary. Hence, these designs are guarded commercial secrets. Therefore, a general and widely used physical model of thyristor is established to simulate the effect of neutron irradiation on the electrical characteristics of thyristor devices, the 2D model of the device and doping concentration as shown in Fig. 8.

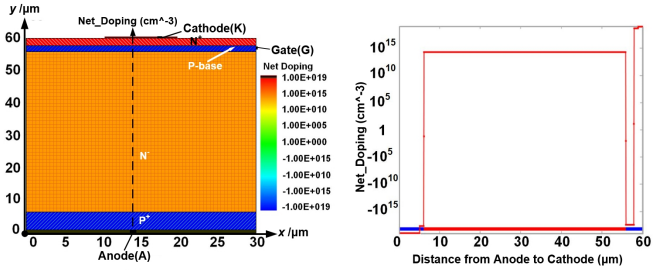

(a) (b)

Fig. 8. (Color online) Simulation model of thyristor. (a) 2D model. (b) doping concentration.

The mathematical models mainly include basic models and key models. The basic model include drift diffusion model, poisson equation, continuity equation, ohmic contact electrical boundary, etc.The key models include mobility model, collision ionization model, bulk defect model, etc. After determining the physical parameters of the thyristor model, the basic semiconductor equations can be solved numerically by combing the initial conditions and the boundary conditions, and the electrical parameters under the specific bias voltage are solved.

The blocking characteristic of the thyristor are shown in Fig. 9a. It can be seen that the leakage current of the thyristor increases sharply when the reverse voltage is 350 V. When U_{AK} = -400 V, the 2D electric field distribution is shown in Fig. 9b, the main electric field falls in the N-region.

The on-state characteristic of the thyristor is shown in Fig. 10. It can be seen that when the triggering voltage V_G = 0.5 V, the thyristor does not trigger on, while when V_G = 1 to 5 V, the thyristor triggers on.

The comparison of the blocking characteristics of thyristor before and after neutron irradiation are shown in Fig. 11 and

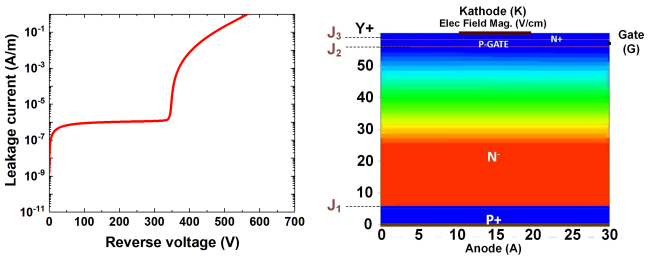

Fig. 9. (Color online) Blocking characteristic. (a) I-V characteristic. (b) 2-D electric field distribution (U_{AK} = -400 V).

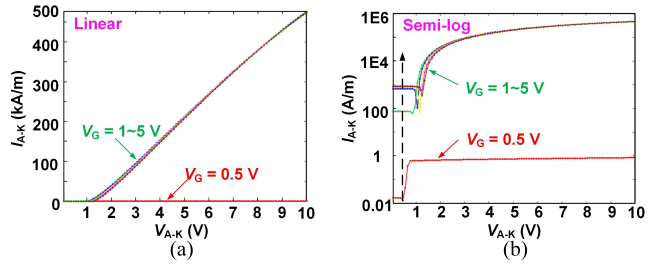

Fig. 10. (Color online) Conducting characteristic. (a) Linear. (b) Semi-log.

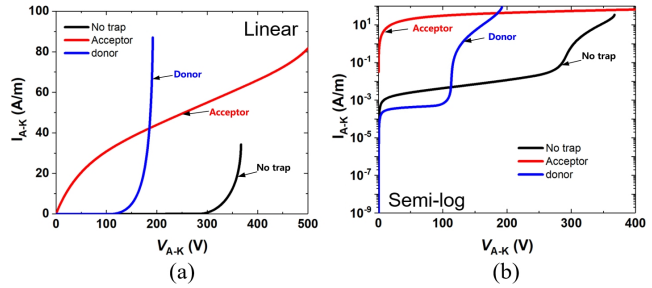

Fig. 11. (Color online) I_{DRM} of irradiated thyristor (donor-type and acceptor-type defect). (a) Linear. (b) Semi-log.

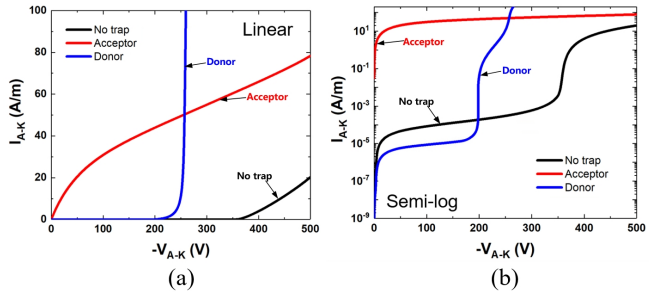

Fig. 12. (Color online) I_{RRM} of irradiated thyristor (donor-type and acceptor-type defect). (a) Linear. (b) Semi-log.

Fig. 12. It can be seen that when the thyristor is subjected to the same voltage, the forward and reserve leakage current I_{DRM}, I_{RRM} increases under both donor and acceptor defect effects.

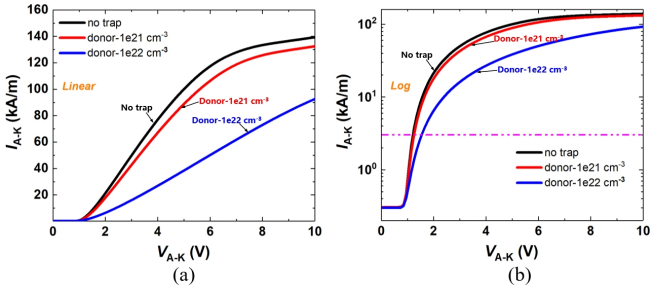

Fig. 13. (Color online) U_{TM} of irradiated thyristor (donor-type defect). (a) Linear. (b) Semi-log.

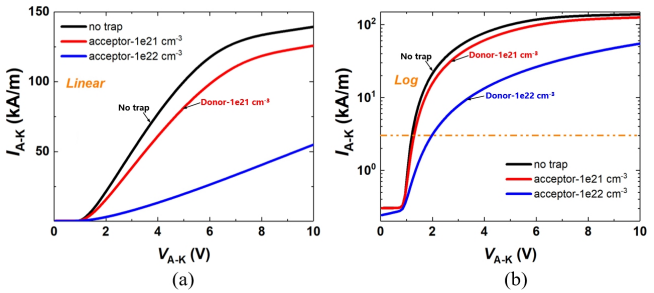

Fig. 14. (Color online) U_{TM} of irradiated thyristor (acceptor-type defect). (a) Linear. (b) Semi-log.

The comparison of on-state characteristics of thyristors before and after neutron irradiation is shown in Fig. 13 and Fig. 14. It can be seen that when the thyristor flows through the same current, the on-state voltage drop U_{TM} increases after irradiation under both donor defect and acceptor defect effects.

The simulation results show that the forward and reverse leakage current and on-state voltage of thyristor increase after neutron irradiation, which is consistent with the theoretical analysis above.

IV. NEUTRON IRRADIATION EXPERIMENT

This paper uses the D-T neutron generator for irradiation, which is based on the accelerator neutron source and affiliated with the China Academy of Engineering Physics (CAEP), Mianyang, China. The experiment is carried out on the K-400 accelerator, using accelerated Deuterium (D) beam to irradiate Tritium (T) target, and D-T reaction occurs, producing fast neutrons with energy of about 14.1 MeV.

To improve the efficiency of neutron irradiation experiment, a new device layout mode, called stepped layout mode is proposed and shown in Fig. 15. Six ABB 5STP 52U5200 thyristor devices are distributed in three spherical spaces with different radii for irradiation, and two thyristors in each radius face the neutron source with anode and cathode, respectively.

According to the neutron calculation report of ITER, the neutron flux rate at QPS could be up to $10^5 n \times cm^{-2} \times s^{-1}$ with local shielding. In this paper, the average neutron flux

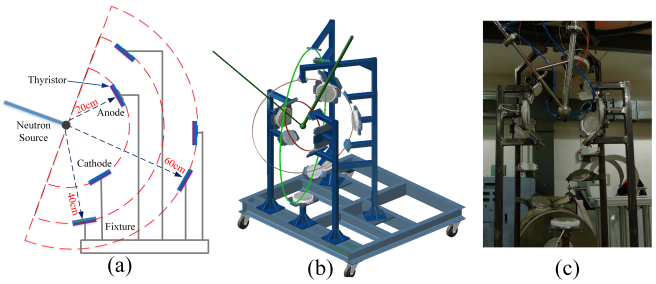

Fig. 15. (Color online) Schematic diagram of neutron irradiation experiment. (a) 2D space distribution. (b) 3D space distribution. (c) Neutron source.

rate is taken as $10^4 n \times cm^{-2} \times s^{-1}$. Assuming that the duty cycle of ITER operating is 0.5, the operating time of a year is estimated as $1.58 \times 10^7 s$, so the neutron flux at QPS could reach $1.58 \times 10^{11} n \times cm^{-2}$. In order to obtain more extreme results, the neutron flux at 20 cm away from the neutron source is set to $4.3 \times 10^{11} n \times cm^{-2}$, which is 2.7 times larger than the actual irradiation environment. Then the output number of the neutron source can be calculated by the following formula.

$$n_{Total} = \phi \times 4\pi r^2 = 2.16 \times 10^{15} n, \tag{35}$$

In the irradiation experiment, the cumulative irradiation time was 95373 s, and the final number of neutrons produced by the D-T neutron generator is $2.55 \times 10^{15} n$ (uncertainty is 4%), which meets the experimental requirement.

In addition, the neutron flux of the devices from near to far is 1:1/4:1/9, and the Cross-sectional area of the irradiated thyristor is 233 cm^2, So the neutron flux and the neutron injection number of the thyristors at each position could be calculated.

As the thyristor stack in QPS is used as the trigger unit of commutation circuit, which is shown in Fig. 1, the temperature of the thyristor is not obvious after flowing through 1 ms/100 kA pulse current. Hence, the electrical parameters that need to be tested when the device temperature is 25 °C are taken as the key test data. The tested thyristor number and location are shown in Table 1.

TABLE 1. The thyristor number and location in 14.1 MeV neutron irradiation experiment.

Location	20 cm	40 cm	60 cm
Neutron Flux	$4.3 \times 10^{11} n/cm^2$	$1.07 \times 10^{11} n/cm^2$	$0.48 \times 10^{11} n/cm^2$
Number	#1 #2	#3 #4	#5 #6

The change of the thyristor each parameter before and after neutron irradiation is shown in Fig. 16. It can be seen that the tested electrical parameters of the thyristors have obvious changes after neutron irradiation. As the thyristors are placed 20 cm, 40 cm and 60 cm away from the neutron source respectively, the neutron flux thyristors received could be calculated, which are $4.3 \times 10^{11} n/cm^2$, $1.07 \times 10^{11} n/cm^2$ and $0.48 \times 10^{11} n/cm^2$ respectively. The forward and reverse leakage current I_{DRM} and I_{RRM}, which represent the blocking characteristic of the thyristor. I_{DRM} increases to 637μA, 528μA and 452.5μA respectively, and I_{RRM} increases to 615.5μA, 458μA and 422.5μA respectively. The on-state voltage drop U_{TM} of the irradiated thyristors at different distances from the neutron source increases from 1.26 V to 4.325 V, 1.84 V and 1.415 V respectively. In addition, the value of Q_{rr} and t_{rr} have a significantly reduce after neutron irradiation shown in Fig. 16d and Fig. 16e, which means the severity of the reverse recovery process is reduced and the duration is shortened after neutron irradiation.

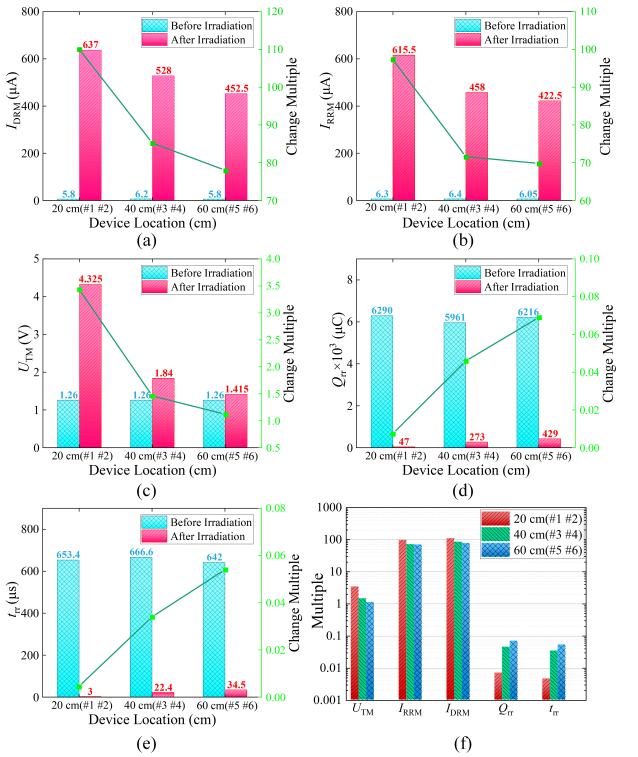

Fig. 16. (Color online) The change of the thyristor each parameter before and after neutron irradiation. (a) Change of I_{DRM}. (b) Change of I_{RRM}. (c) Change of U_{TM}. (d) Change of Q_{rr}. (e) Change of t_{rr}. (f) Change ratio.

In terms of impact degree, the blocking characteristic and reverse recovery characteristic of irradiated thyristor have been seriously affected, which have hundredfold change shown in their key parameters. Meanwhile, the conducting performance of the most severely irradiated thyristors has also decreased by about 3/4, which is shown by the rise of the on-state voltage drop U_{TM}. Moreover, it can be concluded from Fig. 16 that the higher the irradiation flux received by the thyristor, the greater impact on the thyristor electrical parameters, and the greater the performance damage to the thyristor.

V. SIMULATION ANALYSIS OF THE INFLUENCE OF NEUTRON IRRADIATION ON QPS

QPS is a crucial system for not only superconducting magnets, but also fusion device. It is impractical and risky to conduct the irradiation experiments on actual system. With the development of simulation technology and PLECS software, the simulation accuracy has been greatly improved, which could effectively simulate the real QPS electrical performance in normal and operating states. Hence, the simulation method is used to study the impact of neutron irradiation on QPS.

The influence of high-doze neutron irradiation on thyristor stack may bring huge risk of breakdown to QPS in fusion device. Hence, it is of great significance to analyze the impact of neutron irradiation on QPS. By irradiation experiments on QPS is risky and unreasonable, so simulation method for prediction is adopt in this paper. The simplified circuit of QPS in PLECS software and the typical working current waveform are shown in Fig. 17 [36].

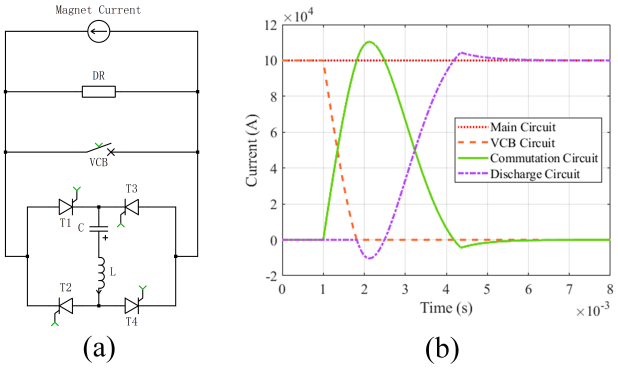

Fig. 17. (Color online) (a) Simplified simulation circuit. (b) Typical current wave of QPS.

According to the results of irradiation experiments, both the static parameters I_{DRM}, I_{RRM}, U_{TM} and dynamic parameters Q_{rr}, t_{rr} all changed significantly after irradiation and may cause the QPS to fail.

The thyristor stack will be turned off and keep in blocking state when QPS in on steady state, in which the capacitor in the commutation circuit shall be charged to the preset voltage. Therefore, the increase of the I_{DRM} may cause the decrease of the capacitor voltage. Once the capacitor voltage drops to a certain value, the pulse current generated by commutation circuit cannot force the current in VCB down to zero, resulting in QPS failure. The larger the I_{DRM}, the short the time for the capacitor voltage drops to the threshold. The breaking failure waveform is shown in Fig. 18. The capacitor does not remain in the reverse blocking state, so the I_{RRM} has almost no obvious impact on QPS.

The thyristor stack will be turned on and keep on-state condition only when the commutation circuit generates the reverse pulse current. Therefore, the change of the U_{TM} will affect the characteristic of the pulse current, which is indicated in Fig. 19. It can be seen that the pulse currents before and after irradiation are almost the same, which suggested that the impact of U_{TM} change on QPS is relatively minuscule.

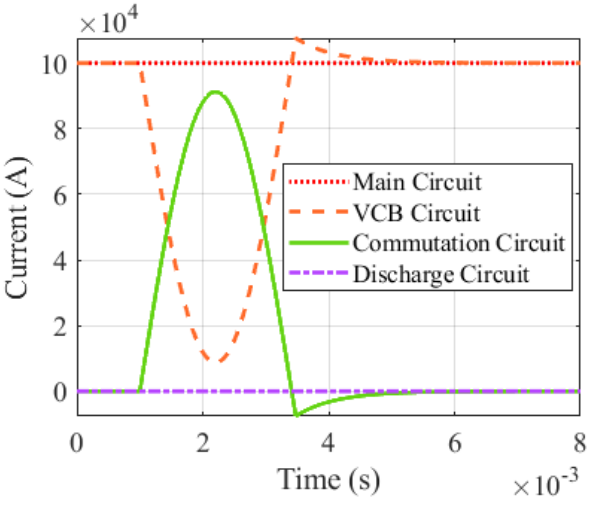

Fig. 18. (Color online) Breaking failure waveform of VCB.

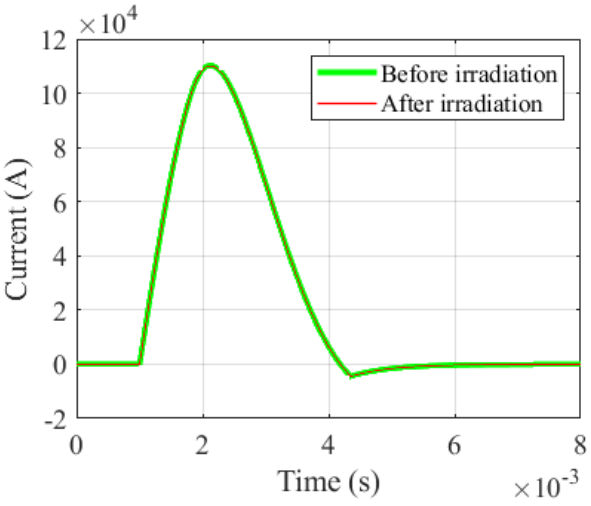

Fig. 19. (Color online) Comparison diagram of the influence of U_{TM} change on the reverse pulse current of QPS.

Theoretical analysis and experiment verification show that the reverse recovery characteristics of the thyristor are significantly changed. The Q_{rr} and t_{rr} are decreased after irradiation, which means that the reverse recovery speed of the irradiated thyristor is accelerated. In QPS, multiple thyristor devices are connected in series to improve the withstand voltage capability. As each thyristor receives different neutron irradiation doze, the change ratio of the reverse recovery speed is different. The voltage waveforms of series connected thyrsitors are shown Fig. 20. It can be seen that before neutron irradiation, the series voltage sharing effect of the four thyristors is good. By contrast, after neutron irradiation, the higher recovery voltage is applied to the thyristor which owns the faster reverse recovery speed. This unexpected event will

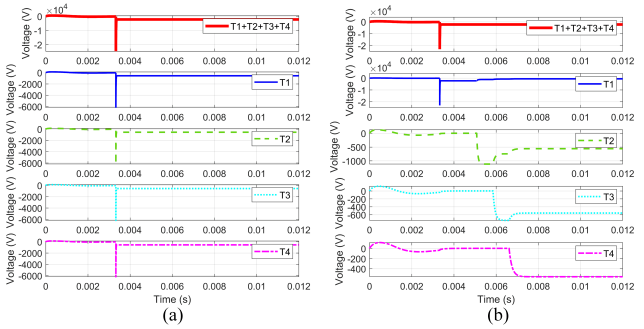

Fig. 20. (Color online) The voltage waveform of the thyristors in reverse recovery process before and after neutron irradiation. (a) Before neutron irradiation. (b) After neutron radiation.

cause the device damage due to overvoltage, leading to the damage of the entire thyristor stack, ultimately resulting in the failure of QPS quench current interruption and transfer actions.

VI. SUMMARY

This paper studies the influence of neutron irradiation on high-power thyristor device in fusion environment. By constructing the relationship between the internal physical structure and external electrical parameters of the thyristor, the effect of neutron irradiation on the thyristor is comprehensively analysis. To verify the correctness of the theoretical analysis, a series of targeted thyristor physical simulations and neutron irradiation experiments carried out. The simulation results and the experiment results indicate that the dynamic and static characteristics of the irradiated thyristors have obviously changed, which is consistent with the theoretical analysis. Also, the effect of irradiated thyristors change on QPS in fusion device is simulated by PLECS software. The simulation results show that the U_{TM} change has little impact on QPS, and the increase of I_{DRM} may lead to VCB breaking failure as the preset voltage decrease of the capacitor in commutation circuit, and inconsistent reverse recovery speed of irradiated thyristors will lead to high reverse voltage in device, which may cause breakdown and reduces the reliability and stability of QPS. In future mature fusion devices, neutrons would be confined in the main engine, the irradiation problem might be greatly improved. In future work, the assessment of the safe operational limits for thyristors in irradiation environment would be deeply studied to further ensure the reliability of the operating thyristors in QPS of Tokamak fusion device, which including irradiation sensitive area localization, the changing relationship between neutron flux and key electrical parameters, and also the degradation threshold of those parameters.

[1] K. Tomabechi, J. R. Gilleland, Yu.A. Sokolov et al., ITER conceptual design. Nucl. Fusion. **31**, 1135 (1991). doi: 10.1088/0029-5515/31/6/011

[2] J. Li, Y. Wan (the EAST team), The Experimental Advanced Superconducting Tokamak. Engineering-Prc. **7**, 1523-1528 (2021). doi: 10.1016/j.eng.2021.10.004

[3] J. Ongena, R. Koch, R. Wolf, H. Zohm, Magnetic-confinement fusion. Nat. Phys. **12**, 398-410 (2016). doi: 10.1038/nphys3745

[4] Mustafa Yiğit, Eyyup Tel, Theoretical determination of (d, n) and (d, 2n) excitation functions of some structural fusion materials irradiated by deuterons. Nucl. Sci. Tech. **28**, 245-253 (2017). doi: 10.1007/s41365-017-0316-6

[5] W. Chen, L. Hu, G. Zhong et al., Study on the gamma rays and neutrons energy response optimization of a scintillating fiber detector for EAST with Geant4. Nucl. Sci. Tech. **34**, 134 (2023). doi: 10.1007/s41365-023-01290-4

[6] W. Zhou X. Fang, J. Fang et al., DC performance and AC loss of cable-in-conduit conductors for International Thermonuclear Experimental Reactor. Nucl. Sci. Tech. **27**, 74 (2016). doi: 10.1007/s41365-016-0061-2

[7] S. Zheng, M. Chen, J. Li et al., Neutronics analysis for the test blanket modules proposed for EAST and ITER. Nucl. Fusion. **47**, 1053-1056 (2008). doi: 10.1088/0029-5515/47/8/040

[8] D. Martin et al., NIU report on radiation issues on electronics in B11. ITER Org., Marseille, France, Tech. Rep. Jun. 2016.

[9] W. Tong, M. Xu, H. Li et al., The Effects of Neutron Irradiation on the Electrical Characteristics of High-power Thyristor. 2023 IEEE 6th International Electrical and Energy Conference (CIEEC) 2362-2365 (2023). doi: 10.1109/ICET55676.2022.9825404

[10] W. Tong, M. Xu, H. Li et al., The conceptual design of upgraded 100 kA quench protection system for CRAFT superconducting magnet. Fusion. Eng. Des. **187**, 113397 (2022). https://doi.org/10.1016/j.fusengdes.2022.113397

[11] W. Zhou, X. Fang, J. Fang et al., Numerical and experimental analysis of AC loss for CFETR CS model coil. Nucl. Sci. Tech. **28**, 142 (2017). https://doi.org/10.1016/j.fusengdes.2022.113397

[12] M. Xu, W. Tong, H. Li et al., Research on Dynamic Voltage Balancing of Series Connected Thyristors in Auxiliary Oscillation Zero-Crossing Circuit. IEEE Trans. Plasma. Sci. **51**, 164-171 (2023). doi: 10.1109/TPS.2022.3231596

[13] M. Xu, H. Li, Z. Song et al., The challenge and solution of overvoltage for 100 kA quench protection system in CRAFT project. Fusion. Eng. Des. **175**, 113001 (2022). doi: https://doi.org/10.1016/j.fusengdes.2022.113001

[14] W. Tong, M. Xu, H. Li et al., 100 kA/10 kV thyristor stack design for quench protection system in CRAFT. Plasma. Sci. Technol. **25**, 055601 (2023). doi: 10.1088/2058-6272/aca8eb

[15] W. Tong, Z. Song, P. Fu et al., Feasibility Analysis of 100 kA DC Commutation Scheme to be Applied in the Quench Protection Unit of CFETR. IEEE Trans. Appl. Supercon. **30**, 1-9 (2020). doi: 10.1109/TASC.2019.2926376

[16] H. Li, Z. Song, S. Wang et al., Study on DC protection switch for superconducting coils in magnetic confinement fusion device. Proc. CSEE, **36**, 233–239 (2016). doi: 10.13334/j.0258-8013.pcsee.161406

[17] C. R. Nobs et al., Computational evaluation of N-16 measurements for a 14 MeV neutron irradiation of an ITER first wall

component with water circuit. Fusion. Eng. Des. **159**, 111743 (2020). https://doi.org/10.1016/j.fusengdes.2020.111743

[18] H. L. Swami et al., A neutronic experiment to support the design of an Indian TBM shield module for ITER. PLASMA SCI TECHNOL. **21**, 6 065601 (2019) https://doi.org/10.1088/2058-6272/ab079a

[19] C. Yin et al., Effect of high-temperature neutron irradiation on fracture toughness of ITER-specification tungsten. PHYS SCRIPTA. **T171**, 014052 (2020) https://doi.org/10.1088/2058-6272/ab079a

[20] Overview of the ITER policy on electronics exposed to radiation.

[21] Overview of the implementing procedure of the ITER policy on electronics exposed to radiation.

[22] J. Prinzie, F. M. Simanjuntak, P. Leroux et al., Low-power electronic technologies for harsh radiation environments. Nat. Electron. **4**, 243-253 (2021). doi: 10.1038/s41928-021-00562-4

[23] D. Li, C. Li, M. Xiao et al., Deconstructing plasma fog collection technology: an experimental study on factors impacting collection efficiency. J. Phys. D: Appl. Phys. **75**, 075201 (2024). doi: 10.1088/1361-6463/ad0ac2

[24] G. Liu, X. Wang, M. Li et al., Effects of high-energy proton irradiation on separate absorption and multiplication GaN avalanche photodiode. Nucl. Sci. Tech., **29**, 139 (2018). doi: 10.1007/s41365-018-0480-3

[25] S. Yue, Z. Chen, Z. Zhang et al., Synergistic Effect of Electrical Stress and Neutron Irradiation on Silicon Carbide Power MOSFETs. IEEE Trans. Electron. Dev. **69**, 3341-3346 (2022). doi: 10.1109/TED.2022.3170539

[26] R. Chen, Y. Liang, J. Han et al., Research on the Synergistic Effect of Total Ionization and Displacement Dose in GaN HEMT Using Neutron and Gamma-Ray Irradiation. Nanomaterials-Basel **12**, 2126 (2022). doi: 10.3390/nano12132126

[27] F. Ravotti, M. Glaser, M. Moll and F. Saigne, BPW34 Commercial p-i-n Diodes for High-Level 1-MeV Neutron Equivalent Fluence Monitoring. IEEE Trans. Nucl. Sci. **55**, 2133-2140 (2008). doi: 10.1109/TNS.2008.2000765

[28] J. Mekki, M. Moll, M. Fahrer, M. Glaser and L. Dusseau, Prediction of the Response of the Commercial BPW34FS Silicon p-i-n Diode Used as Radiation Monitoring Sensors up to Very High Fluences. IEEE Trans. Nucl. Sci. **57**, 2066-2073 (2010). doi: 10.1109/TNS.2010.2044191

[29] C. Liu, C. Yang, W. Chen et al., Experimentally Demonstrating Fast Neutron Irradiation Effect on High-di/dt Switching Characteristics of Insulated Gate Triggered Thyristor for Pulse Power. 2022 IEEE 34th International Symposium on Power Semiconductor Devices and ICs (ISPSD), 177-180 (2022). doi: 10.1109/ISPSD49238.2022.9813637

[30] S. J. Watts, J. Matheson, I. H. Hopkins-Bond et al., A new model for generation-recombination in silicon depletion regions after neutron irradiation. IEEE Trans. Nucl. Sci. **43**, 2587-2594 (1996). doi: 10.1109/23.556840

[31] U. Biggeri, E. Borchi, M. Bruzzi et al., Comparison of radiation damage in silicon detectors induced by pions, protons and neutrons. Il Nuovo Cimento A (1965-1970). **109**, 1351-1358 (1996). doi: 10.1007/BF02773521

[32] T. K. Maiti and C. K. Maiti, Modeling of radiation-induced displacement damage in silicon solar cells: Frenkel defect. 2009 16th IEEE International Symposium on the Physical and Failure Analysis of Integrated Circuits, 647-649 (2009). doi: 10.1109/IPFA.2009.5232562

[33] P. Chen, Radiation Effects on Semiconductor Devices and Integrated Circuits. Beijing, China: National Defense Industry Press, 2005.

[34] E. Liu, B. Zhu, J. Luo, The Physics of Semiconductors 7th Edition. Beijing, China: Publishing House of Electronics Industry, 2017.

[35] W. Tong, H Li, P. Fu et al., Parameter Optimization of Thyristor Snubber Circuit in LSTF Quench Protection System. IEEE Access. **7**, 81257-81265 (2019). doi: 10.1109/ACCESS.2019.2923442

[36] P. Górecki et al., Accurate Computation of IGBT Junction Temperature in PLECS. IEEE Transactions on Electron Devices. **67**, 2865-2871 (2020). https://ieeexplore.ieee.org/document/9093206